

Parity Forbidden Excitations of $\text{Sr}_2\text{CuO}_2\text{Cl}_2$ Revealed by Optical Third-Harmonic Spectroscopy

A. B. Schumacher,* J. S. Dodge,† M. A. Carnahan, R. A. Kaindl, and D. S. Chemla
*Department of Physics, University of California at Berkeley, Berkeley, California 94720 and
 Materials Sciences Division, E. O. Lawrence Berkeley National Laboratory, Berkeley, California 94720*

L. L. Miller

Ames Laboratory and Department of Physics, Iowa State University, Ames, IA 50011

(Dated: October 24, 2018)

We present the first study of nonlinear optical third harmonic generation (THG) in the strongly correlated charge-transfer insulator $\text{Sr}_2\text{CuO}_2\text{Cl}_2$. For fundamental excitation in the near-infrared, the THG spectrum reveals a strongly resonant response for photon energies near 0.7 eV. Polarization analysis reveals this novel resonance to be only partially accounted for by three-photon excitation to the optical charge-transfer exciton, and indicates that an even-parity excitation at 2 eV, with a_{1g} symmetry, participates in the third harmonic susceptibility.

A central theme of condensed matter physics is the problem of treating Coulomb interactions on the electron-Volt scale to determine such low-energy phenomena as the Mott metal-insulator transition, superexchange, and superconductivity. The two-dimensional copper oxide plane has emerged as a model system for studying these phenomena. While excitations at the high-energy scale have been observed in the linear optical spectrum of insulating cuprates, the details of their lineshapes, temperature dependence, and even their assignment has been controversial [1]. In this Letter, we employ nonlinear optical spectroscopy to determine the symmetry and spectrum of both even and odd parity states near the charge-transfer (CT) gap of the model insulating cuprate, $\text{Sr}_2\text{CuO}_2\text{Cl}_2$. Through polarization analysis of the nonlinear optical response, we find evidence for an even parity excitation at approximately 2 eV, with a_{1g} symmetry, and we estimate the magnitude of the dipole matrix element that couples this excitation to the CT exciton. The technique that we describe here is generally applicable to correlated insulators, and should provide valuable input into models of their electronic structure.

The undoped one-layered oxyhalides of the $\text{M}_2\text{CuO}_2\text{X}_2$ ($\text{M} = \text{Ca}, \text{Sr}, \text{Ba}$; $\text{X} = \text{F}, \text{Cl}, \text{Br}$) family are of special interest for studying the excitation spectrum in cuprates. These compounds share the quasi two-dimensional CuO_2 layers which form the structural and electronic basis for high-temperature superconductivity. Unlike their pure oxide counterparts, however, the intervening alkaline earth and halogen elements provide these materials with a very stable stoichiometry. $\text{Sr}_2\text{CuO}_2\text{Cl}_2$ in particular can be obtained in single crystal form with very high quality [2]. It is regarded as an almost ideal realization of a two-dimensional, spin-1/2 Heisenberg anti-ferromagnet at half filling and serves as the test compound for theory

in the low-doping regime.

The most obvious optical feature in the insulating cuprates is the CT gap excitation near 2 eV. Cluster calculations generically predict additional, optically forbidden CT excitations, with a_{1g} (s) or b_{1g} ($d_{x^2-y^2}$) symmetry in $4/mmm$ [3, 4, 5], but presently there is insufficient experimental guidance for selecting an appropriate minimal model [6, 7, 8]. Parity forbidden excitations with ligand field, or dd character, are also expected; these are intraatomic excitations that result directly from strong correlations, in which the hole in the ground state (g) $\text{Cu}(3d_{x^2-y^2})$ orbital is transferred to another Cu orbital of different symmetry.

Large energy-shift laser Raman spectroscopy provided early evidence for the existence and energy spectrum of such excitations, with the assignment of a transition $d_{x^2-y^2} \rightarrow d_{xy}$ at 1.35 eV [9], also identified in optical measurements [10, 11]. From a ligand-field analysis of related peaks in the resonant X-ray Raman spectrum, Kuiper *et al.* have suggested that the $d_{3z^2-r^2}$ (a_{1g}) state should be located at 1.5 eV, but were unable to observe it directly for technical reasons [12]. While a peak in the B_{1g} laser Raman spectrum of some insulating cuprates may be consistent with an assignment to this state, this peak is only observed in T' -phase materials [13].

In our experiment, we completely characterize the THG third order susceptibility tensor elements, $\chi^{(3)}(-3\omega; \omega, \omega, \omega)$, for the Cu-O $\{x, y\}$ -plane of $\text{Sr}_2\text{CuO}_2\text{Cl}_2$. In the space group $I4/mmm$ possessed by $\text{Sr}_2\text{CuO}_2\text{Cl}_2$ the nonlinear susceptibility tensor has two independent elements in the $\{x, y\}$ -plane, $\chi_{xxxx}^{(3)}$ and $\chi_{xyyy}^{(3)}$, which are in general complex. All tensor elements related to $\chi_{xyyy}^{(3)}$ by permutation of the indices are equal, $\chi_{yyyy}^{(3)} = \chi_{xxxx}^{(3)}$, and all other tensor elements are zero. For a driving optical field E at frequency ω , polarized in

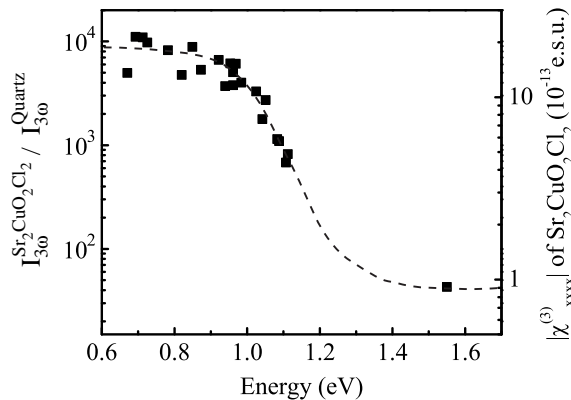


FIG. 1: Third harmonic generation in $\text{Sr}_2\text{CuO}_2\text{Cl}_2$. The left axis shows the relative values of $I(3\omega) \propto |\chi_{xxxx}^{(3)}|^2$. The right scale indicates absolute values for $\text{Sr}_2\text{CuO}_2\text{Cl}_2$. Dashed line: guide to the eye.

the $\{x, y\}$ -plane, the nonlinear polarization is given by

$$\begin{aligned} P_x(3\omega) &= \chi_{xxxx}^{(3)} E_x^3 + 3\chi_{xxyy}^{(3)} E_x E_y^2, \\ P_y(3\omega) &= \chi_{xxxx}^{(3)} E_y^3 + 3\chi_{xxyy}^{(3)} E_x^2 E_y. \end{aligned} \quad (1)$$

Throughout, we take x and y to correspond to coordinates aligned with the crystalline axes of $\text{Sr}_2\text{CuO}_2\text{Cl}_2$, with the z -axis normal to the crystal and in the direction of propagation. It is useful to write the two tensor elements in terms of an amplitude and a phase: $\chi_{xxxx}^{(3)} = \kappa_{xx} e^{i\alpha}$, and $\chi_{xxyy}^{(3)} = \kappa_{xy} e^{i\beta}$, with the phase difference defined as $\delta = \beta - \alpha$.

We first measured the magnitude of the third harmonic susceptibility $|\chi_{xxxx}^{(3)}|$ at room temperature, as a function of fundamental photon energy. These and all other measurements described here were performed with a 250 kHz Ti:sapphire laser amplifier driving an optical parametric amplifier. To account properly for variations in pulse duration and mode profile as the laser wavelength is tuned, we compared the third harmonic intensity $I(3\omega)$ generated in $\text{Sr}_2\text{CuO}_2\text{Cl}_2$ with a quartz reference. We accounted for the $\text{Sr}_2\text{CuO}_2\text{Cl}_2$ absorption at 3ω in the limit $\ell \ll \lambda$, $\Delta k \ell \approx 0$, appropriate here [14]. The $\text{Sr}_2\text{CuO}_2\text{Cl}_2$ samples were cleaved to a thickness of $\ell \sim 100$ nm, and oriented crystallographically with X-ray diffraction. The quartz reference was a thin, $\ell = 150$ μm , c -axis plate, whose absolute nonlinear susceptibility, $\chi_{xxxx}^{(3)}(\text{quartz}) = 3 \times 10^{-14}$ esu, is known independently [15]. The measured relative intensities along with the resulting $|\chi_{xxxx}^{(3)}|$ of $\text{Sr}_2\text{CuO}_2\text{Cl}_2$ are shown in Fig. 1. The spectrum exhibits a broad ≈ 0.5 eV wide resonance at 0.7 eV, varying by more than a factor of 20 over the explored frequency range. Since the susceptibility $\chi^{(3)}(-3\omega; \omega, \omega, \omega)$ involves summation over differ-

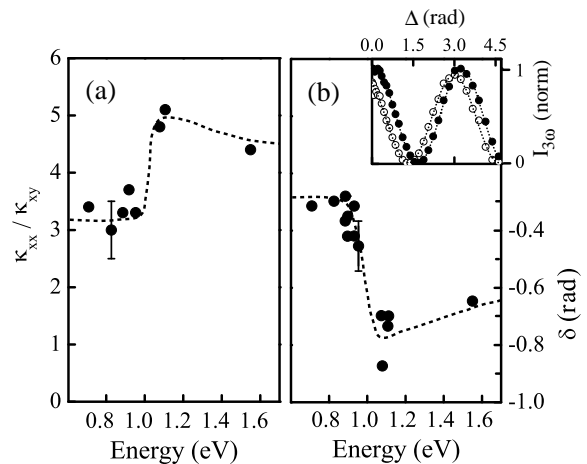


FIG. 2: (a) Relative phase δ and (b) relative magnitude ρ of $\chi_{xxxx}^{(3)}$ and $\chi_{xxyy}^{(3)}$ in $\text{Sr}_2\text{CuO}_2\text{Cl}_2$. The dashed lines are guides to the eye. Inset: Example of a retardance measurement: $I^x(3\omega)$ (filled circles) and $I^y(3\omega)$ (open circles) recorded at $\omega = 0.89$ eV. The dotted lines represent best fits to a \sin^2 function, from which δ and ρ are extracted.

ent intermediate states, the resonance may result from a parity allowed, three-photon transition at $3\omega = 2.1$ eV, a parity forbidden, two-photon transition at $2\omega = 1.4$ eV, or both. All of these possibilities are consistent with previously published results [1].

Our chief experimental results are the spectroscopic measurements of the relative amplitude $\rho = \kappa_{xx}/\kappa_{xy}$ and the relative phase δ of $\chi_{xxxx}^{(3)}$, $\chi_{xxyy}^{(3)}$, shown in Figs. 2(a) and (b), respectively. These data were obtained from polarization-sensitive measurements of the third harmonic optical intensity along each of the two crystalline axes of the sample, $I^{x,y}(3\omega)$, while varying the polarization state of the fundamental laser field. In the experimental geometry used here, the incident field is initially polarized at 45 degrees to the two crystalline axes, then passes through a polarization compensator before entering the sample. The natural axes of the compensator are aligned with those of the crystal, so the polarization state upon entering the sample is given by $\vec{E} = [\hat{x}E + \hat{y}Ee^{i\Delta}]/\sqrt{2}$, where Δ is the compensator retardance. Thus, the nonlinear polarizations $P_x(3\omega)$ and $P_y(3\omega)$ involve controlled mixtures of $\chi_{xxxx}^{(3)}$ and $\chi_{xxyy}^{(3)}$, with Δ as the control parameter, as may be seen through Eq. 1.

As the compensator is adjusted, the THG intensities $I^x(3\omega) \propto |P_x(3\omega)|^2$ and $I^y(3\omega) \propto |P_y(3\omega)|^2$ both oscillate sinusoidally with Δ . Results from a typical measurement, for $\hbar\omega = 0.89$ eV, are shown in the inset of Fig. 2. Straightforward manipulation of Eq. 1 tells us further that the phase offset in Δ between these two intensity curves is δ , and that the minima of $I^{x,y}(3\omega, \Delta)$ are

offset from zero by $\kappa_{xy}(\rho - 3)$. From a series of such measurements at various laser frequencies, we obtain the dispersion of the relative amplitude $\rho(\omega)$ and relative phase $\delta(\omega)$, shown in Figs. 2(a) and (b), respectively. These data show that $\rho(\omega)$ and $\delta(\omega)$ both undergo clear, step-like changes at about 1 eV. Since these are relative quantities, we can derive the model-independent conclusion that as the photon energy crosses $\hbar\omega \approx 1$ eV, the transition dipole elements involved in $\chi_{xxxx}^{(3)}$ and $\chi_{xxyy}^{(3)}$ connect states with different symmetry. We show below that this can only be the result of an excitation with a_{1g} symmetry at 2 eV.

The tensor elements of the nonlinear susceptibility are given by

$$\chi_{ijkl}^{(3)}(-3\omega; \omega, \omega, \omega) = \frac{N}{\hbar^3} \mathcal{P}_I \sum_{n=1}^8 \mathcal{K}_{ijkl}^{(n)}(-3\omega, \omega, \omega, \omega), \quad (2)$$

where the intrinsic permutation operator \mathcal{P}_I applies to the last three tensor indices $\{jkl\}$ [16]. The eight terms $\mathcal{K}^{(n)}$ correspond to different summations over intermediate states. The dominant term in our experiment is $\mathcal{K}^{(1)}$, which may be written

$$\mathcal{K}_{ijkl}^{(1)} = \sum_{\nu_1, \nu_2, \nu_3} \frac{\mu_{g\nu_1}^i \mu_{\nu_1\nu_2}^j \mu_{\nu_2\nu_3}^k \mu_{\nu_3g}^l}{(\Omega_{\nu_1g} - 3\omega)(\Omega_{\nu_2g} - 2\omega)(\Omega_{\nu_3g} - \omega)}, \quad (3)$$

where $\{\nu_1, \nu_2, \nu_3\}$ are the intermediate states, $\mu_{\nu_1\nu_2}^i = \langle \nu_1 | \mu^i | \nu_2 \rangle$ are dipole matrix elements along the direction \hat{r}_i , and each $\Omega_{\nu_\ell g} = \omega_{\nu_\ell g} - i\gamma_{\nu_\ell g}$ is a complex frequency associated with a transition from the ground state g to an intermediate state ν_j . Individual terms in Eq. 3 may be one-, two-, or three-photon resonant, or it may contain double or triple resonances, depending on the location and symmetry of the states ν_ℓ . If the product of matrix elements in Eq. 3 is to be nonzero, symmetry requires both that ν_1 and ν_3 transform as e_u in $4/mmm$, and that ν_2 transforms as a_{1g} (z^2), a_{2g} ($x^3y - xy^3$), b_{1g} ($x^2 - y^2$) or b_{2g} (xy). Moreover, the summation over all possible permutations in Eq. 2 leads to additional cancellations, so that those terms in which ν_2 transforms as a_{2g} or b_{2g} do not contribute to the THG signal. Consequently, the even-parity states which contribute to the THG signal are exclusively those with a_{1g} or b_{1g} symmetry.

To evaluate the role of these intermediate states in the measured third harmonic spectrum, we compare our results from $\text{Sr}_2\text{CuO}_2\text{Cl}_2$ to the results of a phenomenological, independent-level model, commonly used in nonlinear optics [16]. We assume that the excited states are independent levels, each with its own energy, dephasing rate, and symmetry. To obtain a realistic estimate of the matrix elements, excited state energies, and decay rates of the odd-parity states, observed in conventional linear optics, we performed a fit of four lorentzian functions to the experimentally determined absorption spectrum [17, 18]. By attributing each of these lorentzians

to a different state η_n , where n ranges from one to four, we obtain from the fit the energies E_n , dephasing rates γ_n , and dipole matrix elements μ_{gn}^x connecting each state η_n to the ground state. These parameters are listed in Table I. We emphasize that the parameters used here are chosen merely to yield a good description of the *linear* susceptibility, and subsequently remain fixed for the nonlinear susceptibility calculation using Eq. 2.

The results of this model calculation are shown as solid lines in Fig. 3. Panel (a) shows that the absolute magnitude of $\chi_{xxxx}^{(3)}$ exhibits a peak near 0.7 eV, roughly one third of the energy of the first odd-parity excited state η_1 of the model, as expected from a three-photon resonance. Panels (b) and (c) show that the relative amplitude and phase are completely flat as a function of frequency, with the value of the amplitude ratio ρ fixed at three, while the phase difference δ is fixed at zero. This is the behavior expected of a spherically symmetric nonlinear hyperpolarizability [19]. It should be noted that in this case, the relative quantities ρ and δ are entirely insensitive to the details of the model parameters, because their values are determined by symmetry. We find that in general, if the ground state possesses b_{1g} symmetry, then *any* set of excited states containing only b_{1g} and e_u symmetries will display this overall, spherically symmetric hyperpolarizability, over the entire frequency spectrum. The model, however, does give the right order of magnitude for $|\chi_{xxxx}^{(3)}|$. In the case of $\text{Sr}_2\text{CuO}_2\text{Cl}_2$, then, the magnitude of the nonlinear susceptibility is dominated by a three-photon resonance to CT excited states, and is only weakly enhanced by two-photon resonances to even-parity states [20].

While the overall magnitude and shape of the resonance in $\chi_{xxxx}^{(3)}$ is explained well with only the optically allowed CT excited states, the structure that we observe in δ and κ_{xx}/κ_{xy} implies the involvement of excitations with different symmetries. As we have seen, the only other states that may contribute to the THG signal are those with a_{1g} symmetry. Moreover, when these states are included in Eq. 2, the transitions to the a_{1g} and b_{1g} intermediate states will interfere. Since $\langle x|x|a_{1g} \rangle = \langle y|y|a_{1g} \rangle$, and $\langle x|x|b_{1g} \rangle = -\langle y|y|b_{1g} \rangle$, this interference will exhibit different behavior in $\chi_{xxxx}^{(3)}$ and $\chi_{xxyy}^{(3)}$, to produce exactly the deviations from spherical

TABLE I: Energies E_n , dephasing rates γ_n , and matrix elements μ_{gn}^x , μ_{en}^x used in the model calculations described in the text.

η_n	E_n (eV)	γ_n (eV)	μ_{gn}^x (10^{-18} esu)	μ_{en}^x (10^{-18} esu)
η_1	1.96	0.25	1.86	3.72
η_2	2.44	1.75	4.00	0.80
η_3	4.00	5.75	4.70	0.94
η_4	5.00	5.75	4.11	0.82

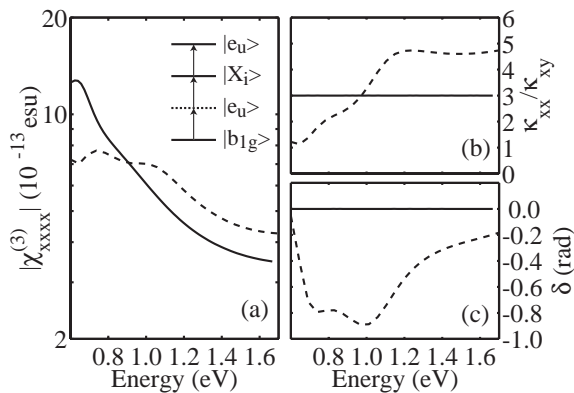


FIG. 3: Comparison of two model calculations for $\chi^{(3)}$: (a) magnitude, (b) relative amplitude ρ , and (c) relative phase δ . The inset shows the level scheme assumed in the model, with $|X_i\rangle$ the two-photon states of interest. In all panels, solid lines indicate that only the virtual excitation to $|X_1\rangle = |b_{1g}\rangle$ is included. Dashed lines indicate the addition of a resonant state at 2.0 eV, $|X_2\rangle = |a_{1g}\rangle$.

symmetry that we observe. Thus, we extend our model calculation by adding an excitation with a_{1g} symmetry at 2.0 eV. The additional matrix elements μ_{en}^x coupling this excited state to the four odd-parity excited states are given in Table I. Remarkably, the results shown as dashed lines in Figs. 3 (b,c) are in close agreement with the experiment, both in sign and in magnitude. There is considerable uncertainty in the parameters obtained from this simplified model, so the error on our estimate of the energy of the a_{1g} excitation may be as large as 0.4 eV. However, even with this error, the midinfrared range is clearly excluded [11], and the symmetry of the state is unambiguously determined through this analysis.

Finally, we turn to the assignment of this excitation. Symmetry-allowed alternatives include a CT exciton, a Cu dd excitation, and coupled modes, such as an exciton-phonon (i.e., $a_{1g} \in e_u \otimes e_u$). It is likely, however, that *all* of these excitations are active in this range, and are strongly mixed. This proposal is supported by the anomalously broad Urbach tail observed at low temperatures in $\text{Sr}_2\text{CuO}_2\text{Cl}_2$, which has been explained recently by a model that involves strong coupling between the charge-transfer gap excitation and another, optically forbidden, excitation nearby in energy [18]. Electronic structure calculations place both the Cu dd and the a_{1g} CT excitons near 2 eV [3, 5, 12], and both modes would be expected to couple strongly to the e_u CT exciton via phonons. As our theoretical understanding of these excitations grows, our estimate of the matrix elements μ_{en}^x may provide a further test of this scenario.

In summary, we have determined the spectrum of the full THG nonlinear optical susceptibility tensor for $\text{Sr}_2\text{CuO}_2\text{Cl}_2$, using both absolute measurements against

a standard reference and relative measurements based on polarization analysis. The dominant feature in the absolute measurement is a peak at $\hbar\omega \sim 0.7$ eV, which can be explained as a three-photon resonance to the CT gap. The relative measurements show that an additional, optically forbidden state near 2 eV participates in the THG spectrum, and that this state possesses a_{1g} symmetry. Both the symmetry and the energy of this state are consistent with a mixed mode involving both a $d_{x^2-y^2} \rightarrow d_{3z^2-r^2}$ transition and a coupled CT-exciton-phonon mode. These measurements were performed with fundamental frequencies well away from resonance, in contrast to previous Raman work, and the relative measurements have enabled the estimation of the optical matrix elements coupling the even-parity state to the CT gap excitation. In general, both Raman and THG spectroscopy are different cuts through the three-dimensional frequency space that $\chi^{(3)}$ may probe. Further development of nonlinear optical spectroscopy will provide a more complete determination of these and other optical excitations.

This work was supported by the U.S. Department of Energy under Contracts No. DE-AC03-76SF00098 and W-7405-Eng-82. Fellowships from the German National Merit Foundation (ABS), and the Deutsche Forschungsgemeinschaft (RAK) are gratefully acknowledged, as is the assistance of Z. Rek, Z. Hussain and X. Zhou for their assistance in orienting the $\text{Sr}_2\text{CuO}_2\text{Cl}_2$ platelet. We thank G. A. Sawatzky and M. V. Klein for their comments on the manuscript.

* also Institut für Angewandte Physik, Universität Karlsruhe, 76128 Karlsruhe, Germany

† Present address: Department of Physics, Simon Fraser University, Burnaby, BC V5A 1S6, Canada

- [1] M. A. Kastner et al., *Rev. Mod. Phys.* **70**(3), 897 (1998).
- [2] L. L. Miller et al., *Phys. Rev. B* **41**, 1921 (1990).
- [3] M. E. Simón et al., *Phys. Rev. B* **54**, R3780 (1996).
- [4] F. C. Zhang and K. K. Ng, *Phys. Rev. B* **58**, 13520 (1998).
- [5] E. Hanamura, N. T. Dan, and Y. Tanabe, *J. Phys.: Condens. Matter* **12**, L345 (2000).
- [6] Y. Y. Wang et al., *Phys. Rev. Lett.* **77**, 1809 (1996).
- [7] M. Z. Hasan et al., *Science* **288**, 1811 (2000).
- [8] A. Schülzgen et al., *Phys. Rev. Lett.* **86**, 3164 (2001).
- [9] R. Liu et al., *Phys. Rev. Lett.* **71**, 3709 (1993).
- [10] J. P. Falck et al., *Phys. Rev. B* **49**, 6246 (1994).
- [11] J. D. Perkins et al., *Phys. Rev. Lett.* **71**, 1621 (1993).
- [12] P. Kuiper et al., *Phys. Rev. Lett.* **80**, 5204 (1998).
- [13] D. Salamon et al., *Phys. Rev. B* **51**, 6617 (1995).
- [14] D. S. Chemla and J. Zyss, *Nonlinear optical properties of organic molecules and crystals* (Academic Press, New York, 1987).
- [15] J. P. Hermann, *Opt. Commun.* **9**(1), 74 (1973).
- [16] R. W. Boyd, *Nonlinear Optics* (Academic Press, Inc., San Diego, 1992), 9th ed.

- [17] H. S. Choi et al., Phys. Rev. B **60**, 4646 (1999).
[18] R. Löwenich et al., Phys. Rev. B **63**, 235104 (2001).
[19] P. D. Maker and R. W. Terhune, Phys. Rev. **137**,
A803 (1965).
[20] H. Kishida et al., Nature **405**, 929 (2000).